Developmental Biology 379 (2013) 28–37

Contents lists available at SciVerse ScienceDirect

Developmental Biology

journal homepage: www.elsevier.com/locate/developmentalbiology

TAF13 interacts with PRC2 members and is essential for *Arabidopsis* seed development

Matias Lindner [a], Sara Simonini [a], Maarten Kooiker [a,1], Valeria Gagliardini [b,c], Marc Somssich [d], Mareike Hohenstatt [d], Rüdiger Simon [d], Ueli Grossniklaus [b,c], Martin M. Kater [a,*]

[a] *Dipartimento di BioScienze, Università degli Studi di Milano, Via Celoria 26, 20133 Milan, Italy*
[b] *Institute of Plant Biology, University of Zürich, Zürich, Switzerland*
[c] *Zürich-Basel Plant Science Center, University of Zürich, Zürich, Switzerland*
[d] *Institut für Genetik, Heinrich-Heine-Universität, Universitätstr 1, 40225 Düsseldorf, Germany*

ARTICLE INFO

Article history:
Received 13 October 2012
Received in revised form
28 February 2013
Accepted 1 March 2013
Available online 15 March 2013

Keywords:
Seed
Arabidopsis
Polycomb Repressive Complex 2
Endosperm
Gene regulation

ABSTRACT

TBP-Associated Factors (TAFs) are components of complexes like TFIID, TFTC, SAGA/STAGA and SMAT that are important for the activation of transcription, either by establishing the basic transcription machinery or by facilitating histone acetylation. However, in *Drosophila* embryos several TAFs were shown to be associated with the *Polycomb* Repressive Complex 1 (PRC1), even though the role of this interaction remains unclear. Here we show that in *Arabidopsis* TAF13 interacts with MEDEA and SWINGER, both members of a plant variant of *Polycomb* Repressive Complex 2 (PRC2). PRC2 variants play important roles during the plant life cycle, including seed development. The *taf13* mutation causes seed defects, showing embryo arrest at the 8–16 cell stage and over-proliferation of the endosperm in the chalazal region, which is typical for *Arabidopsis* PRC2 mutants. Our data suggest that TAF13 functions together with PRC2 in transcriptional regulation during seed development.

Introduction

Transcription of protein encoding genes by RNA polymerase II (Pol II) requires the formation of the Preinitiation Complex (PIC), which is composed of Pol II and several General Transcription Factors (GTFs), such as TFIIA, TFIIB, TFIID, TFIIE, TFIIF and TFIIH (Thomas and Chiang, 2006). The first step of PIC assembly is the recognition of core promoter elements, which is mainly driven by TFIID. This general transcription factor complex is composed of the TATA-box Binding Protein (TBP) and several highly conserved TBP-Associated Factors (TAFs). In *Arabidopsis thaliana* a total of 21 different *TAF* genes were identified (Lago et al., 2004; Lawit et al., 2007). Several TAFs share the presence of a Histone Fold Domain (HFD) (14 out of 21 in *Arabidopsis*), a fundamental motif for protein–protein and DNA–protein interactions that is important for TFIID structure and function. The TAF proteins facilitate TFIID binding to different core promoter elements not necessarily containing the TATA-box (Basehoar et al., 2004). Besides their ability to bind core promoter elements, TAFs also function as co-activators interacting with specific transcription factors to modulate basal transcription machinery activity (Thomas and Chiang, 2006).

According to their role in the basal transcription machinery, TAFs were expected to be required for accurate transcription of all genes. However, in yeast it was shown that each TAF regulates the expression of a limited subset of genes, ranging from 3% to 61% of the genes (Shen et al., 2003; Lee et al., 2000). Moreover, tissue-specific TAFs was were reported in animals (Voronina et al., 2007; Hiller et al., 2001). The specificity of TAFs in the regulation of distinct subsets of genes is in accordance with results obtained in *Arabidopsis*. For instance, the *taf1* mutant showed decreased levels of chlorophyll accumulation, light-induced mRNA levels, and acetylation of histone H3 in light-responsive promoters, suggesting an involvement of *TAF1* in light signal transduction (Bertrand et al., 2005). Moreover, in young *taf1* mutant leaves 9% of the genes showed an alteration in their expression. Other examples are *Arabidopsis TAF6*, which regulates pollen tube growth (Lago et al., 2005), and *TAF10*, which controls meristem activity, leaf development and osmotic regulation (Tamada et al., 2007; Gao et al., 2006).

TAFs are also components of other complexes different from TFIID, such as TFTC (TBP-free TAF_{II}-containing complex), TFTC-related PCAF/GCN5 complexes, the Spt–Ada–Gcn5 acetyltransferase (SAGA) complex, SAGA-like complexes (SLIK), the Spt3–TAF9–GCN5L acetylase (STAGA) complex, and the Small TAF complex

* Corresponding author. Fax: +39 02 50315044.
E-mail address: martin.kater@unimi.it (M.M. Kater).
[1] Present address: Plant Ecophysiology, Institute of Environmental Biology, Utrecht University, Padualaan 8, 3584 CH Utrecht, The Netherlands.

0012-1606/$ - see front matter © 2013 Elsevier Inc. All rights reserved.
http://dx.doi.org/10.1016/j.ydbio.2013.03.005

(SMAT), all of which do not contain TBP (Wieczorek et al., 1998; Grant et al., 1998; Ogryzko et al., 1998; Martinez et al., 1998; Demeny et al., 2007). The majority of these complexes possess histone acetylase (HAT) activity, meaning that they are involved in gene activation (Thomas and Chiang, 2006). Surprisingly, six different TAFs were pulled-down with several components of *Polycomb* Repressive Complex 1 (PRC1) from *Drosophila* embryos (Saurin et al., 2001). *Polycomb* Group (PcG) proteins act in multi-protein complexes to maintain a repressive state of gene expression, controlling several important developmental processes. In particular, PRC1 is a well-characterized multi-protein complex able to mono-ubiquitinylate lysine 119 of histone H2A (H2AK119ub), generally recognized as a transcriptional repressive mark able to modify chromatin structure. In *Drosophila*, two other PcG containing complexes were identified named PRC2 (involved in histone H3 lysine 27 trimethylation, H3K27me3) and Pho Repressive Complex (PhoRC), which has sequence specific DNA-binding activity.

In *Arabidopsis*, most homologs of PRC1 components are absent but PRC1-like activities were recently demonstrated (Bratzel et al., 2010; Chen et al., 2010). In contrast, several variants of plant PRC2 are well characterized, and the core components of PRC2 are highly conserved in protein structure and function when compared to animals (reviewed in Schatlowski et al., 2008; Hennig and Derkacheva, 2009; Holec and Berger, 2012; Bemer and Grossniklaus, 2012). In *Arabidopsis*, three different variants of PRC2 were described, acting in different processes and developmental stages during the plant life cycle: the FERTILIZATION INDEPENDENT SEED (FIS) complex acting in the female gametophyte and during seed development, the VERNALIZATION (VRN) complex acting in the vernalization response, and the EMBRYONIC FLOWERING (EMF) complex preventing precocious flowering and regulating flower development. These complexes share common subunits, such as FERTILIZATION-INDEPENDENT ENDOSPERM (FIE) and MULTICOPY SUPPRESSOR OF IRA1 (MSI1), and complex-specific components: FIS2 and MEDEA (MEA) or SWINGER (SWN) in the FIS-PRC2; VRN2 and CURLY LEAF (CLF) or SWN in the VRN-PRC2, and EMF2 and CLF or SWN in the EMF-PRC2 (Kohler et al., 2003a; Chanvivattana et al., 2004; Wood et al., 2006; De Lucia et al., 2008). Mutations in any of the components of the FIS-PRC2, with the exception of SWN, lead to autonomous seed development in the absence of fertilization, and to seed abortion with embryo and endosperm overgrowth when fertilization occurs (Ohad et al., 1996, 1999; Chaudhury et al., 1997; Grossniklaus et al., 1998; Luo et al., 1999; Kohler et al., 2003a).

Here, we characterize *TAF13* of *Arabidopsis* and show that, like mutants of the *fis* class, *taf13* mutants have endosperm overgrowth, suggesting a possible link between TAF13 and FIS-PRC2.

Materials and methods

Plant material and growth conditions

Arabidopsis thaliana accession Columbia was used as the wild type and grown at 22 °C in short-day (8 h light/16 h dark) or long-day (16 h light/8 h dark) conditions. Mutations disrupting *TAF13* (*At1g02680*), *taf13-1* (SALK_119642), *taf13-2* (SALK_016938), *taf13-3* (SALK_024774), *taf13-4* (SALK_078709), and the *atfh5-2* mutant (SALK_044464) were obtained from the European Arabidopsis Stock Centre (NASC) (Alonso et al., 2003). The *mea-8* mutant was supplied by NASC (SAIL_55_B04). The *mea-2* mutant was described by Grossniklaus et al. (1998), the *pMEA*::*GUS* transgenic line by Baroux et al. (2006), the *pPHE1*::*GUS* line by Kohler et al. (2003b), the *pFUS3*::*GUS* line by Makarevich et al. (2006). Plants carrying *pFIS2*::*GUS* were kindly provided by A. Chaudhury (Luo et al., 2000). The enhancer trap line KS117 was kindly provided by F. Berger (Sorensen et al., 2001).

Nicotiana benthamiana plants were grown for 4 weeks in a greenhouse under controlled conditions prior to agroinfection.

Genotyping, segregation and complementation analysis

Genotyping of *TAF13*, *taf13-1*, *taf13-2*, *taf13-3*, *taf13-4*, *MEA*, *mea-8*, *AtFH5* and *Atfh5-2* plants was done by PCR using the primers reported in Supplementary Table 1.

For complementation experiments the *TAF13* genomic region plus 2.5 Kb upstream the transcription start site was cloned into the pDONOR207 vector (Life Technologies; for primers see Supplementary Table 1) and then recombined into pGW::EGFP (pGreenII; Hellens et al., 2000). The obtained construct was used to transform *taf13-2*/*TAF13* plants using the floral dip method (Clough and Bent, 1998) through the *Agrobacterium tumefaciens* strain GV3101 pMP90. Transformed seeds were selected with BASTA.

GUS assay and microscopic analysis

The GUS assay was performed as described (Liljegren et al., 2000).

To analyze seed development in wild-type and mutant plants, seeds at different developmental stages were cleared overnight using a solution composed of 160 g chloral hydrate (C-8383; Sigma-Aldrich), 100 ml water, and 50 ml glycerol. The samples were observed using a Zeiss Axiophot D1 microscope equipped with DIC optics. Images were captured on an Axiocam MRc5 camera (Zeiss) using the Axiovision program (version 4.1).

For *pTAF13*::*TAF13-GFP* and KS117-GFP analysis, siliques at different developmental stages were dissected in water and observed using the Leica DM 6000 microscope.

In situ hybridization and expression analysis

In situ hybridization analysis was performed as described in Dreni et al. (2011). The antisense probe corresponds to a 321-bp fragment at the 5' end of the *TAF13* cDNA. The accumulation of *TAF13*, *MEA*, and *mea-2* transcripts were measured using quantitative real-time RT-PCR as described by Baroux et al. (2006). Quantitative analysis of transcript levels were carried out using Sybr Green or Taqman real-time PCR assays (Applied Biosystem). Three technical replicates were performed for each independent cDNA sample ($n=3$), and the specificity and amount of the unique amplification product were determined according to the manufacturer's instructions (Applied Biosystems). *MEA* and *mea-2* transcripts were measured to confirm the wild-type or mutant background of the samples. In all experiments, transcript levels were normalized to the level of *ACTIN1*.

Protein interaction and pull-down assays

The yeast two-hybrid assays were performed at 28 °C in the yeast strain AH109 (Clontech), using the co-transformation technique (Egea-Cortines et al., 1999). The interactions were tested on selective YSD medium lacking leucine, tryptophan, adenine or/and histidine, supplemented with different concentrations of 3-amino-triazole (5, 10 mM 3-AT). *TAF13*, *MEA*, *VRN2* and *MSI1* were cloned in the pGBKT7 and pGADT7 vectors (Clontech), passing through pENTR/D-TOPO (Life Technologies). *CLF* lacking the SET-domain and *EMF2* constructs were kindly provided by Dr. Chanvivattana (Chanvivattana et al., 2004). *FIE*, *SWN*, and *TFL2* were cloned into the pGBKT7 vector (Clontech), passing through the pENTR223 vector (Life Technologies), whereas the *SWN* lacking the SET-domain and *TFL2* lacking the chromodomain constructs were cloned into pCR8-GW-Topo (Life Technologies). The pull-down

assay has been performed according to Brambilla et al. (2007), however for this study we prepared protein A and protein G magnetic beads (Life Technologies) to which Anti-*c-Myc* antibodies (Santa Cruz Biotechnology) were attached. *MEA* was fused to the GST-tag and *TAF13* to the c-MYC-tag (present respectively in the pGEX-2T and in the pGADT7 vectors). The primers used are reported in Supplementary Table 1. For Western blot analysis we used the anti-GST antibody (GEHealthcare).

Transient gene expression in N. benthamiana leaves

The destination plasmids pABindGFP, pABindmCherry, and pABindFRET used in this study were described in Bleckmann et al. (2010). To create receptor fusions, coding regions of *TAF13*, *MEA* and *SWN* were amplified and recombined into pENTR/D-TOPO (Life Technologies) according to the manufacturer's instructions. For the fusion of SWN lacking the SET-domain (C-terminal part) it was recombined in PDONR207 (Clontech) from the corresponding yeast two-hybrid vector pGBKT7 (Clontech).

The *Agrobacterium tumefaciens* strain GV3101 pMP90 was transformed with expression clones plus the silencing suppressor p19 (Voinnet et al., 2003). Leaves of 4-week-old *N. benthamiana* plants were infiltrated with the culture. Transgene expression was induced 48 to 96 h after infiltration with 20 mM b-estradiol + 0.1% Tween 20 and analyzed within 4–24 h.

FRET and confocal microscopy

Epidermis cells were examined with a 40×1.3 numerical aperture Zeiss oil-immersion objective using a Zeiss LSM 510 Meta confocal microscopy system. GFP was excited with a 488-nm argon laser with emission detection through the meta-channel at 497–550 nm. mCherry was excited at 561 nm using a diode, and emission was detected at 572–636 nm via the meta-channel. E_{FRET} was measured via GFP fluorescence intensity increase after photobleaching of the acceptor mCherry. Frame size was kept constant at 256×256 pixels, with a pixel time of 2.55 μs per pixel. A region of interest around the Plasma Membrane (PM) was bleached after five detection frames with 100% laser intensity of the 561-nm diode and 120 iterations. Fifteen frames were recorded after photobleaching. The GFP fluorescence intensity change was analyzed around the PM in the region of interest. Only measurements with less than 10% GFP intensity fluctuations before acceptor bleaching were further analyzed. The percentage change of the GFP intensity directly before and after bleaching was analyzed as E_{FRET}=(GFP after−GFP before)/GFP after $\times 100$. FM464 (Invitrogen) staining was performed at a final concentration of 20 μM for 5–20 min. A minimum of 15 measurements were performed for each experiment. Significance was analyzed using the Student's *t* test.

Results

Identification of taf13 mutant lines

Arabidopsis thaliana TAF13 was identified based on the primary amino acid sequence homology with TAF13 proteins of other organisms (Lago et al., 2004). The protein is mainly composed of a HFD and RT-PCR experiments demonstrated expression of its mRNA in roots, rosette leaves, and inflorescences. We obtained 4 different T-DNA insertion lines for *TAF13* from the SALK collection (Supplemental Fig. 1). A preliminary analysis of these lines revealed plants homozygous for the T-DNA insertion for all mutant alleles except for *taf13-2*, which has an insertion in the third exon. A subsequent segregation analysis using a selfed *taf13-2* heterozygous line showed a ratio of 82 wild-type:133 heterozygous plants and the complete absence of plants homozygous for the T-DNA insertion. These data indicate that the segregation ratio of wild-type *versus* heterozygous mutant plants is approximately 1:2 (χ^2=2.251; p=0.05), which suggests that the T-DNA insertion in the *taf13-2* mutant results in a recessive embryo lethal phenotype. This suggests that *TAF13* is an essential gene for embryo development in *Arabidopsis*. Based on the position of the T-DNA insertion and the presence of homozygous mutant plants, all other *taf13* alleles we obtained were not considered null alleles and were not analyzed further.

To investigate the presence of possible gametophytic defects in the *taf13-2* mutant, reciprocal crosses between the heterozygous *taf13-2* mutant and wild-type plants were performed. The segregation ratios obtained from these crosses were 1:1, both using plants heterozygous for *taf13-2* as the female (102 wild-type:90 heterozygous, χ^2=0.75; p=0.05) or the male parent (140 wild-type:132 heterozygous, χ^2=0.24; p=0.05), indicating normal gametophyte development and functionality.

To demonstrate that the observed mutant phenotype was caused by the loss of *TAF13* activity, a complementation test was performed using a genomic fragment including 2577 bp 5' of the transcription start site and 1292 bp covering the coding region. In this construct the *TAF13* stop codon was removed to fuse the *TAF13* open reading frame with the *EGFP* reporter gene. Heterozygous *taf13-2* mutant plants were transformed with this construct and in the subsequent generations transgenic plants homozygous for the transgene were selected. Self-fertililzation of these plants that were heterozygous for the *taf13-2* mutation showed normal Mendelian segregation of the mutant allele, and homozygous *taf13-2* mutants were obtained. These findings indicate that the seed phenotype was complemented by the *TAF13* gene construct, evidencing that the observed *taf13-2* phenotype was indeed due to loss of *TAF13* activity. Furthermore, this experiment also showed that the TAF13–EGFP fusion protein has normal biological activity.

Loss of TAF13 activity affects seed development

The *taf13-2* transmission and segregation analysis revealed that seed development is affected in this mutant. Compared to the wild type, where 98% of the developing seeds were normal, siliques of *taf13-2* heterozygous plants contained 76.1% of normally developed green seeds and 23.9% of seeds (n=1301) that were delayed in their development, appeared white (embryo arrested prior to chloroplast biosynthesis) (Fig. 1A and B), and eventually aborted becoming brown and shrunken (Supplementary Fig. 1). Based on the segregation analysis and the percentage of aborted seeds we predict that the delayed seeds correspond to the *taf13-2* homozygous mutants.

To characterize seed defects in *taf13-2* plants in more detail, we analyzed cleared whole-mount seeds by differential interference contrast (DIC) microscopy (Fig. 1C–L). Immediately after pollination, all seeds in heterozygous *taf13-2* siliques were undistinguishable from the wild type (Fig. 1C and H). During later stages of seed development, *taf13-2* seeds showed a delay in development and eventually arrested at the 8- to 16-cell embryo stage, with a few exceptions arresting at earlier stages. In particular when the majority of the seeds had reached the globular stage, 31% of the seeds showed embryos composed of 1–8 cells (n=150), although the endosperm developed normally (Fig. 1D and I). At later stages of development, most of the *taf13-2* mutant embryos had 8–16 cells but also showed a delayed development of the endosperm as compared to normal siblings, even though endosperm development was not arrested. When wild-type seeds were at the torpedo/walking stick stage (Fig. 1E), the endosperm of 24.5% *taf13-2* mutant seeds appeared cellularized (Fig. 1L), presented an

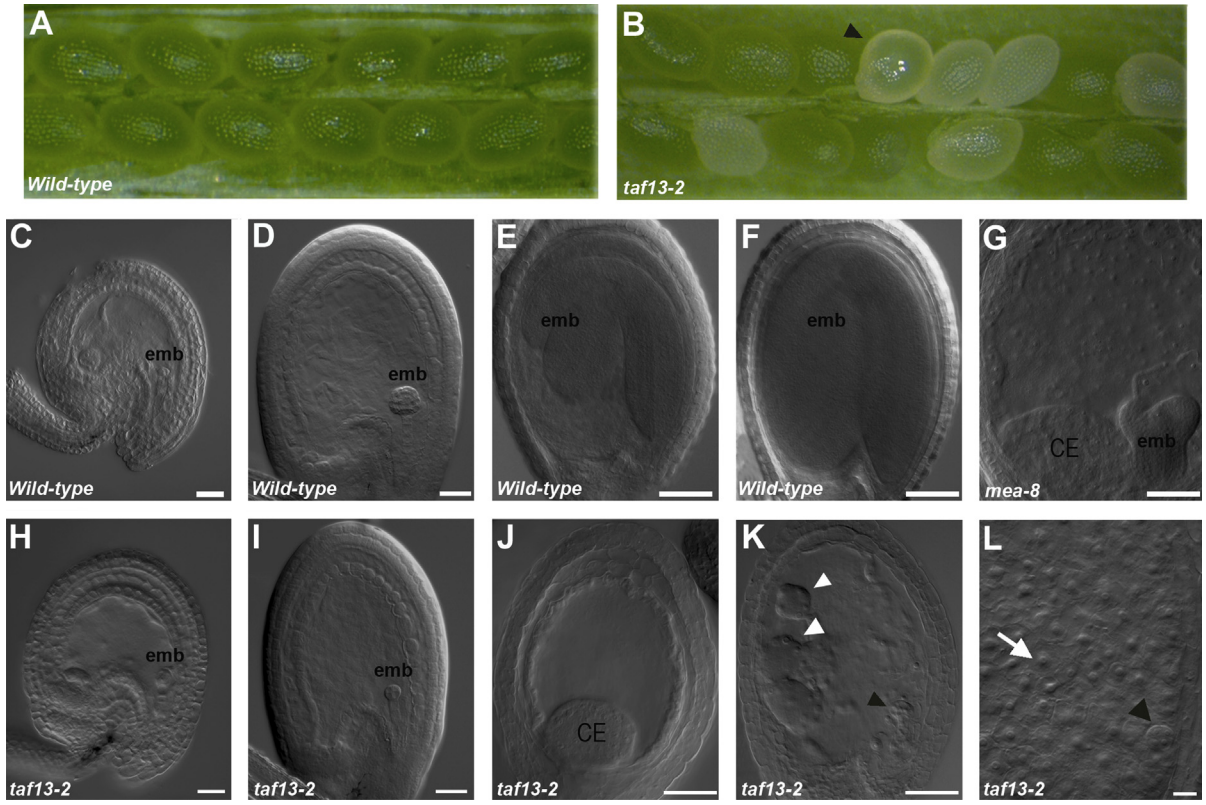

Fig. 1. Analysis of the *taf13* mutant seeds. (A, B) Seeds in siliques at 7 Days After Pollination (DAP) from (A) wild-type and (B) *TAF13*/ *taf13-2* mutant plants, in which seeds delayed in development can be observed (black arrowhead). (C–F) Wild-type seed development: (C) zygote stage embryo, (D) globular stage embryo, (E) walking stick stage embryo, and (F) cotyledon stage embryo. (G) *mea-8* mutant phenotype, with enlarged chalazal endosperm and an over-proliferating heart stage embryo. (H–L) *taf13-2* seed development: (H) zygote stage embryo. When wild-type siblings reach the globular stage and later on, *taf13-2* seeds are blocked at 8–16 cells (I) with an enlarged chalazal endosperm (J), ectopic cyst formation (K, white arrowhead), and a degenerating eight-cells embryo (K and L, black arrowhead) are visible. White arrow in (L) shows a cell of cellularized endosperm. Scale bars 10 μm in C and H; 20 μm in D and I; 50 μm in G; 100 μm in E, F, J, K and L. Emb=embryo; CE=chalazal endosperm.

over-proliferated chalazal region, and in some cases ectopic chalazal cysts ($n=424$) (Fig. 1J and K). In these seeds the embryo degenerated (Fig. 1L and K) or was not visible. Consequently in mature siliques all *taf13-2* seeds were aborted.

The enlarged endosperm in the chalazal region, as we observed it in *taf13-2* mutant seeds, was previously reported for the *Arabidopsis fis* class of mutants (Ohad et al., 1996; Chaudhury et al., 1997; Grossniklaus et al., 1998; Vinkenoog et al., 2000; Sorensen et al., 2001; Kohler et al., 2003a). Cleared seeds derived from *mea-8* female gametophytes were analyzed to compare it with the *taf13-2* mutant phenotype (Fig. 1G). Apart from the enlarged endosperm and the ectopic chalazal cysts observed in both mutants, there were also some differences between them. In *fis* class mutants, embryos over-proliferate and arrest at the heart/torpedo stage while their endosperm does not cellularize; these phenotypes were not observed in *taf13-2* seeds.

TAF13 expression during seed development

According to publically available microarray data, *TAF13* is expressed throughout the plant life cycle at medium levels in all tissues (Hruz et al., 2008). The highest expression levels were detected in the chalazal endosperm with relatively high levels in all seed tissues. To analyze *TAF13* expression in more detail during seed development, we performed an *in situ* hybridization analysis using a gene-specific antisense probe (Fig. 2A–E). *TAF13* transcripts were detected early after fertilization in the zygotic embryo (Fig. 2A, white arrowhead) and free endosperm nuclei (Fig. 2A, black arrowhead). A strong signal was also observed in the integuments, which became weaker at globular stage, when *TAF13* expression was still detectable in embryo (Fig. 2B, white arrowhead) and endosperm (Fig. 2B, black arrowhead). Expression remained visible in the embryo at the heart and torpedo stage (Fig. 2C and D). The chalazal endosperm displayed a signal comparable to the one observed in the embryo (Fig. 2C). At maturity, transcripts were mainly detected in the embryo epidermis and in the vascular tissue, whereas the signal in the integuments was strongly reduced (Fig. 2E). All negative controls with a sense probe showed no detectable signal in any of the samples (Supplementary Fig. 2).

TAF13 protein expression was investigated through confocal microscopy analysis using the *pTAF13::TAF13-GFP taf13-2* line (Fig. 2F–L). In these plants the *taf13* phenotype is complemented confirming that the TAF13-GFP chimeric protein is fully functional in plants.

The expression profile of the TAF13-GFP protein was similar to the mRNA profile observed by *in situ* hybridization: the signal is nuclear and persistent throughout the embryo during all the developmental stages: zygote (Fig. 2F), globular (Fig. 2G), heart (Fig. 2H) and torpedo (Fig. 2I). Interestingly, later at the torpedo stage (Fig. 2J), TAF13-GFP is not only localized in the nuclei but also at the plasma membrane (Figs. 2K and L, arrowheads) both in the cotyledons and in the young radicle, suggesting an intriguing post-translational regulatory mechanism.

MEA and FIS2 are normally expressed in taf13-2 mutant seeds

The FIS-PRC2 is a multi-protein complex, mainly active during female gametophyte and seed development, and is composed of four core subunits: FIE, MSI1, and the ovule/seed specific components FIS2

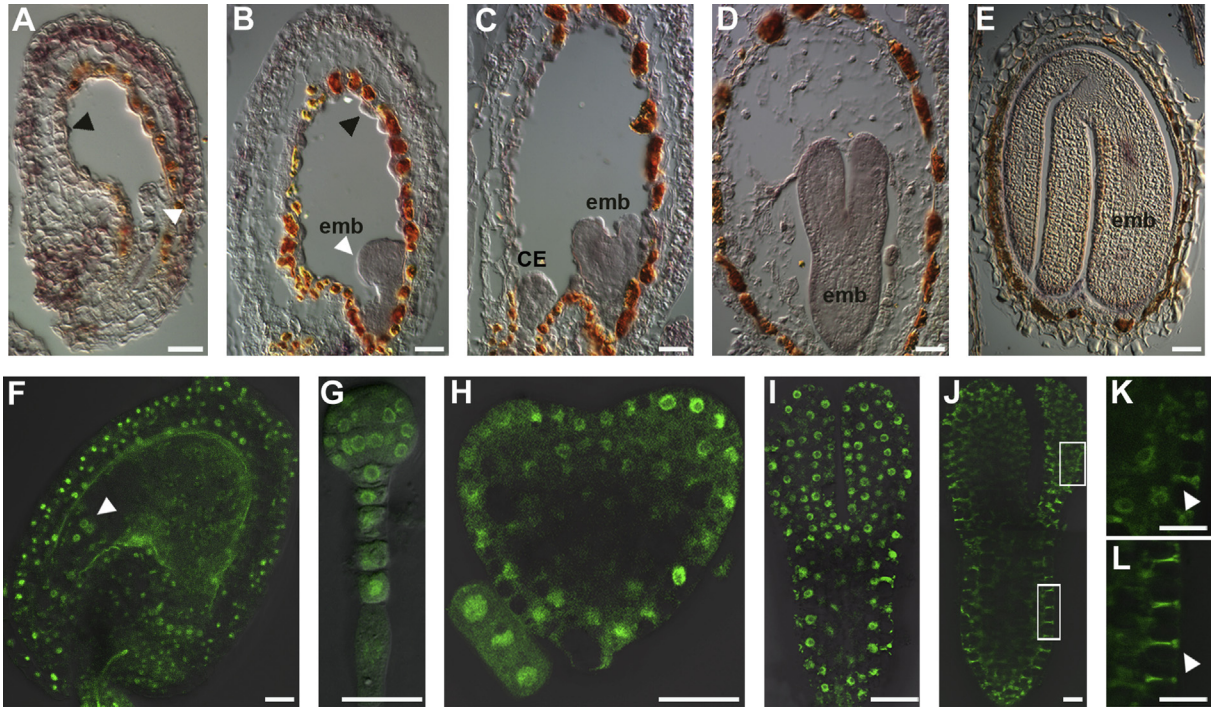

Fig. 2. *TAF13* expression during *Arabidopsis* seed development. (A–E) *In situ* hybridization of zygote to cotyledon stages using an anti-sense *TAF13* RNA probe. Zygote stage embryo (A) with signal in integuments, endosperm (black arrowhead), and embryo (white arrowhead); globular stage embryo (B) in which the signal becomes weaker in integuments but still persists in the embryo (white arrowhead) and endosperm (black arrowhead); heart stage embryo (C) with signal in the chalazal endosperm; walking stick stage embryo (D) cotyledon stage embryo (E). (F–L) TAF13-GFP expression during embryo development in *pTAF13*::*TAF13-GFP taf13* plants. (F) Zygote stage embryo with clear nuclear signal (arrowhead); (G) globular stage, (H) heart-stage, (I) torpedo stage with nuclear signal. (J) Later during the torpedo stage, the expression pattern of TAF13-GFP changes and a clear GFP signal is detected in the nuclei and plasma membrane of cotyledonary tissue (K, arrowhead), whereas in the young radicle TAF13-GFP is mainly localized at the plasma membrane (L, arrowhead). White empty boxes in (J) correspond to the magnification in (K) and (L). Emb=embryo; CE=chalazal endosperm. Scale bars 20 μm.

and MEA. The expression patterns of *FIS2* and *MEA* have been analyzed by GUS assays using *pFIS2*::*GUS* and *pMEA*::*GUS* plants (Luo et al., 2000; Spillane et al., 2004; Baroux et al., 2006). It was shown that after fertilization GUS activity of *pFIS2*::*GUS* is detectable in free endosperm nuclei and subsequently decreases drastically before cellularization, when the signal is observed only in chalazal endosperm nuclei. *pMEA*::*GUS* expression resembles that of *FIS2* except for a more diffuse staining around endosperm nuclei. Compared to the endosperm, only low levels of GUS activity were observed in embryos (Luo et al., 2000; Spillane et al., 2004; Baroux et al., 2006; Raissig et al., 2011), and *MEA* transcripts were detected in the egg cell and in embryos from the zygote to heart stage by *in situ* hybridization (Vielle-Calzada et al., 1999; Spillane et al., 2007).

We decided to analyze *MEA* and *FIS2* expression profiles in the *taf13-2* mutant because of the enlarged chalazal endosperm observed in this mutant, which is a typical characteristic of *fis* mutant seeds. This similarity in phenotype suggests that *TAF13* might be involved in the regulation of *FIS2* and/or *MEA*. To test this hypothesis *taf13-2* plants were crossed with *pFIS2*::*GUS* and *pMEA*::*GUS* plants. The F2 plants heterozygous for *taf13-2* and homozygous for the *pFIS2*::*GUS* or *pMEA*::*GUS* constructs were assayed for GUS activity during seed development. This showed that in 95.3% of the seeds ($n=310$) until the globular stage *pFIS2*::*GUS* expression profiles were normal and identical in all seeds (Fig. 3A–C). After this stage, in a small fraction of *pFIS2*::*GUS* seeds (4.4%; $n=180$), GUS staining was detected in cellularized endosperm nuclei of both wild-type and *taf13-2* in contrast with previous results (Luo et al., 2000). The enlarged endosperm chalazal region in *taf13-2* mutant seeds displayed normal *FIS2* expression (Fig. 3D). In heterozygous *taf13-2 pMEA*::*GUS* plants expression was observed in 84.6% seeds up to the pre-globular stage in all the embryo sacs of wild-type and in the *taf13-2* mutant seeds ($n=247$) (Fig. 3E, F). When *taf13-2* siblings reached the heart stage, the percentage of seeds that still expressed the GUS reporter decreased to 22.8% ($n=259$), a fraction likely representing the *taf13-2* mutant seeds that were delayed in their development. In these mutant seeds, GUS expression remained present throughout the embryo sac, especially in the chalazal endosperm (Fig. 3G). *MEA* expression was still detectable in cellularized endosperm (Fig. 3H), in contrast with previous results (Luo et al., 2000). The slight differences of our wild-type *pFIS2*::*GUS* and *pMEA*::*GUS* expression profiles with those previously published (Luo et al., 2000), might be explained by different plant growth conditions or different GUS assay and/or clearing protocols.

TAF13 is normally expressed in mea-2 seeds

The experiments described above indicate that TAF13 does not regulate *MEA* or *FIS2* expression. Another explanation for the similarity of the *fis* and *taf13* chalazal endosperm phenotypes is that *TAF13* may be a target of the FIS-PRC2 in seeds. Several studies were performed for genome-wide PRC2 target gene identification in *Arabidopsis*. Whole-genome H3K27me3 regions were identified in seedlings (Zhang et al., 2007; Oh et al., 2008) and in endosperm (Weinhofer et al., 2010). The *TAF13* locus appears in none of these studies as a potential PRC2 target. However, the potential regulation of *TAF13* by FIS-PRC2 may be indirect and repressive functions of MEA outside the context of the FIS-PRC2 have been proposed (Baroux et al., 2006). Therefore, we decided to test *TAF13* expression levels in *mea-2* mutant seeds. Plants homozygous for *mea-2* were pollinated with wild-type pollen and seeds were collected from 0 to 4 DAP. As a control, the same experiment was done with the reciprocal cross (wild-type plants pollinated with *mea-2* homozygous pollen). The paternal copy of *MEA* is normally not expressed; therefore, 100% of the collected seeds derived from a *mea-2* homozygous mother lack *MEA* activity. RNA was extracted

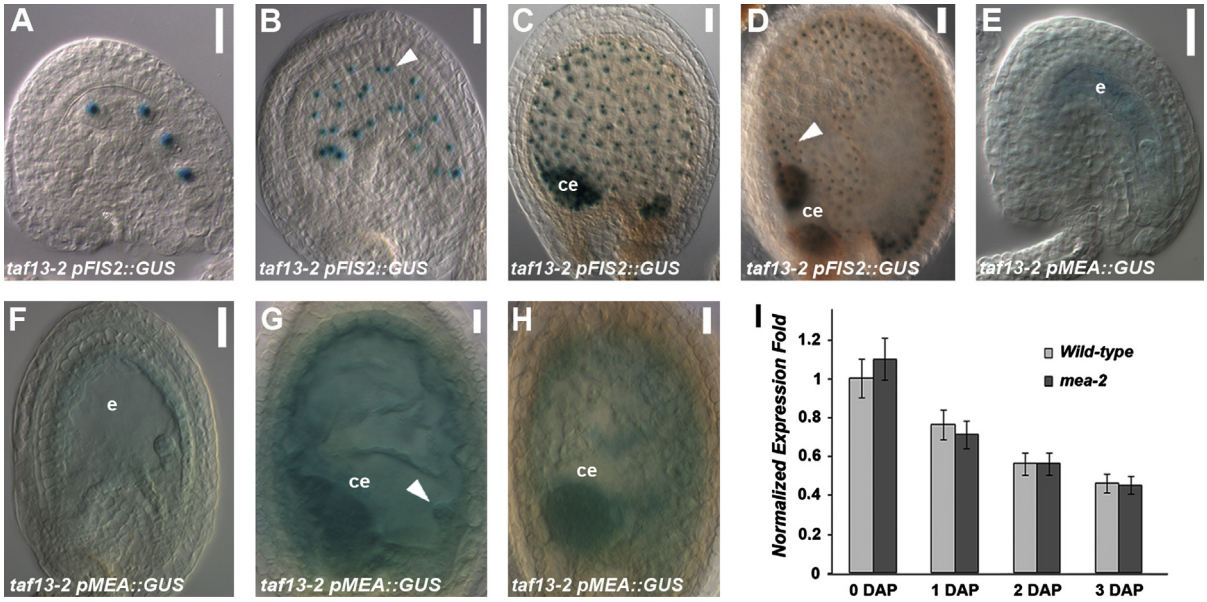

Fig. 3. Analysis of regulatory interactions between *TAF13*, *FIS2* and *MEA*. (A–D) *pFIS2*::*GUS* expression in *taf13-2* seeds. (A) FIS2-GUS is correctly expressed after fertilization. (B) After several mitotic divisions of free endosperm nuclei (arrowhead), the FIS2-GUS expression pattern remains comparable to the wild type. (C) Chalazal endosperm shows strong GUS expression. (D) Cellularized endosperm displays GUS staining also in the chalazal region (arrowhead). (E–H) *pMEA*::*GUS* expression in *taf13-2* seeds. (E) MEA-GUS is correctly expressed after fertilization. (F) MEA-GUS staining is evident throughout the embryo sac at the eight cells embryo stage. (G) Uncellularized endosperm showing MEA-GUS expression in the degenerating embryo (arrowhead). (H) Cellularized endosperm displays GUS activity mainly in the chalazal region. (I) Quantification of *TAF13* transcripts in ovules and developing seeds derived from wild-type and *mea-2* mutant embryo sacs. *TAF13* expression levels are not altered in *mea-2* mutant seeds. Transcripts were quantified before fertilization in entire gynoecia containing unfertilized ovules (0 DAP), and after fertilization in developing fruits following hand pollination (1–4 DAP). Transcript levels were normalized to *ACTIN1*; average and standard deviation of triplicate quantifications are shown. Ce=chalazal endosperm; e=endosperm. Scale bars 20 μm.

and *TAF13* expression levels were analyzed by quantitative real-time PCR. The *TAF13* expression levels were the same in seeds of *mea-2* homozygous plants crossed with wild-type pollen and seeds obtained from the reciprocal control crosses, suggesting that *TAF13* is neither a direct nor an indirect target of MEA and FIS-PRC2 (Fig. 3I).

TAF13 interacts with MEA and SWN

To further investigate a possible link between *TAF13* and the *FIS* class gene functions, we tested for physical interactions between TAF13 and the FIS proteins. Yeast 2-hybrid assays were performed using different PcG proteins, including MEA and SWN, FIE, and MSI1, which are core components of the FIS-PRC2 (Table 1). Among the PcG proteins that were tested for interaction with TAF13, positive results were obtained with MEA and SWN, which are two out of the three SET domain proteins of *Arabidopsis* with homology to Enhancer of zeste [E(z)], the sole H3K27 methyltransferase in *Drosophila*. Curiously, the truncated version of SWN (lacking the C-terminal SET domain, involved in histone methyltransferase activity) only showed a weak interaction with TAF13. We also used the SET domain protein CLF as GAL4 DNA Binding Domain (BD) fusion protein in these interaction studies, which resulted in auto-activation of the reporter gene. This made it impossible to monitor interactions in this configuration. We did not initiate other experiments to test CLF as Activation domain (AD) fusion since CLF is not playing a role during seed development. In contrast to *CLF*, *SWN* has a partially redundant role with *MEA* in pre-fertilization events (Wang et al., 2006), so we decided to focus our attention also on this interaction. The only component of the PRC1-like complex of *Arabidopsis* that was tested for interaction with TAF13 was TFL2, both with the full-length protein and a truncated version, lacking the chromodomain; neither of which showed an interaction (Table 1).

To confirm the yeast 2-hybrid data, we conducted FRET experiments in *Nicotiana benthamiana* leaves. TAF13, MEA, full-length SWN and the truncated SWN protein were all C-terminally fused with GFP and mCherry, and used as a FRET pair. FRET efficiency (E_{FRET}) was measured as the percentage of change in GFP (donor) expression after photobleaching of mCherry (acceptor). An E_{FRET} of ≤4% was considered as background noise (previously described in Bleckmann et al., 2010). As a negative control we tested TAF13 interaction with LBD15 (LOB Domain-containing protein 15), a nuclear localized protein. The E_{FRET} of both pairs TAF13-GFP/LBD15-mCherry and TAF13-mCherry/LBD15-GFP were under the set background noise threshold (Fig. 4A). Unfortunately, we were not able to transiently express some of the fusion proteins, in particular MEA-GFP, MEA-mCherry and SWN-mCherry, probably due to folding problems in the C-terminal part of the protein. However, the pairs TAF13-mCherry/SWN-GFP and TAF13-mCherry/SWN-SET domain-GFP reached E_{FRET} values of around 30%, which is far above the background noise, confirming a strong interaction between TAF13 and SWN (Fig. 4B and C). The combination of TAF13-GFP/SWN-SET domain-mCherry has an E_{FRET} value equal to 2,11%. Folding of SWN-SET domain-mCherry or TAF13-GFP can be impaired, resulting in an increased distance between the fluorophores or, alternatively, concentration effects can explain why this combination does not show E_{FRET} values comparable to the ones obtained with their counterparts.

These results show that TAF13 is able to interact with SWN in two independent protein interaction assays. Since the interactions with MEA could only be tested in yeast, we decided to test this interaction by performing a pull-down assay. TAF13-cMYC and MEA-GST were expressed in *E. coli*, purified, and tested for an *in vitro* interaction three times using different concentration ratios of both proteins. With this approach we obtained a weak but detectable band of MEA-GST in the bound fraction (Supplementary Fig. 3), suggesting that TAF13 is able to interact with MEA *in vitro*, although the larger amount of MEA-GST remained in the not-bound

Table 1
Yeast two-hybrid assay results. TAF13 fused with the GAL4 Activation Domain (pGADT7 [AD]) was tested for interaction with several PcG proteins fused to the GAL4 DNA Binding Domain (pGBKT7 [BD]). Empty vectors pGBKT7 (GAL4 BD fusion vector) and pGADT7 (GAL4 AD fusion vector) were used to test auto-activation of reporter genes. 1=yeast growth in YSD drop-out–W–L–H; 2=yeast growth in YSD drop-out–W–L–H–A; 3=yeast growth in YSD drop-out–W–L–H+5 mM 3-AT; 4=yeast growth in YSD drop-out–W–L–H+10 mM 3-AT.

	pGBKT7	TAF13	FIE	MSI1	MEA	SWN	SWN-SET	CLF-SET	VRN2	EMF2	TFL2	TFL2-chromo
pGADT7	–	–	–	–	–	–	–	1 2 3	–	–	–	–
TAF13	–	1 2	–	–	1 2 3 4	1 2 3 4	1 2	1 2 3	–	–	–	–

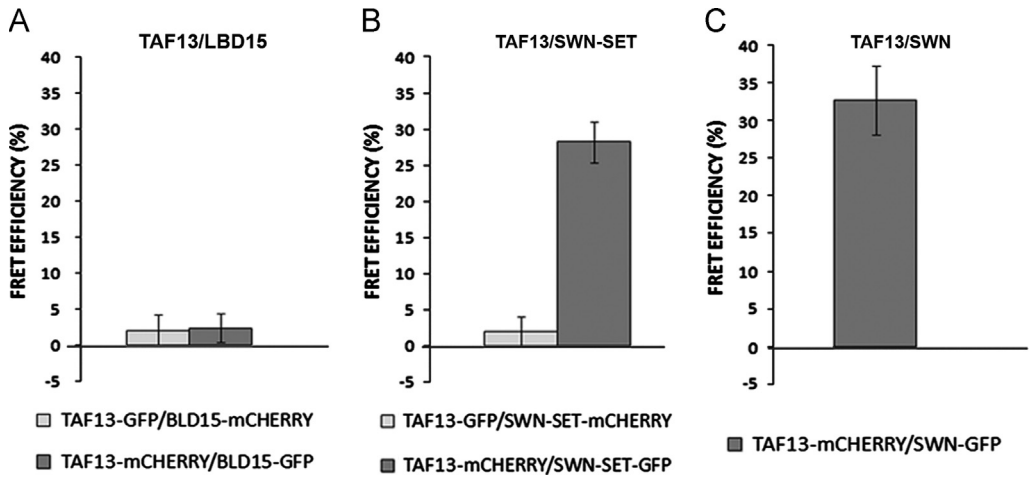

Fig. 4. TAF13 interacts with MEA and SWN. (A) TAF13 interaction tested with LBD15 as negative control. (B) TAF13 interaction tested with the truncated version of SWN lacking the SET domain. (C) TAF13 interaction tested with SWN.

fraction (Supplementary Fig. 3). In conclusion, taken together these interaction data suggest that TAF13 interacts with the two histone-methyltransferases of FIS-PRC2.

PRC2 targets are normally expressed in the taf13-2 mutant

One of the known FIS-PRC2 targets is the plant formin *AtFH5*, encoding an actin nucleator factor involved in cytokinesis (Ingouff et al., 2005). The expression of this gene during seed development is altered in *fis* mutants, in which ectopic expression is observed throughout the endosperm as compared to the normal expression of *AtFH5*, which is restricted to the chalazal endosperm at the heart stage of embryogenesis (Sorensen et al., 2001). The *atfh5-1* and *atfh5-2* mutants display a delay in endosperm cellularization and a reduction of the chalazal endosperm. Interestingly, both double mutants, *atfh5-1 mea-6* and *atfh5-2 mea-6*, do not present the typical overgrowth of the endosperm in the chalazal region that is observed in the *mea* single mutant, suggesting that this characteristic depends on the ectopic expression of *AtFH5* (Fitz Gerald et al., 2009). Since TAF13 seems to interact with MEA and *taf13-2* also presents an enlarged chalazal region, we decided to test whether *AtFH5* is mediating this phenotype. Therefore, we crossed the *taf13-2* heterozygous mutant with the *atfh5-2* mutant. We analyzed seed development in *taf13-2*/*TAF13*; *atfh5-2*/*atfh5-2* F2 plants and found that 21.3% of the seeds (n=320) have the *taf13-2* mutant phenotype with the typically enlarged chalazal endosperm (data not shown). As a control, we also analyzed the seeds of a *mea-8*/*MEA*; *atfh5-2*/*atfh5-2* double mutant and, in contrast with the data from Fitz Gerald et al. (2009), we still observed the enlarged chalazal endosperm typical for *mea* in 48.8% of the seeds (n=240) (Supplementary Fig. 4). Since *taf13-2* is in the Columbia background we used the *atfh5-2* and *mea-8* alleles for our analysis because they are in the same background. The different genetic backgrounds might explain the phenotypic difference between the previously published *mea-6*/*mea-6*; *atfh5-2*/*AtFH5* and our *mea-8*/*MEA*; *atfh5-2*/*atfh5-2* double mutants, or, alternatively, this difference might be due to the distinct *mea* alleles used. Based on our results, we conclude that *taf13* and *atfh5* do not interact genetically, however since we also did not confirm the previously published interaction between *mea* and *atfh5* in Columbia, results might be different in other genetic backgrounds.

To test a possible role of *TAF13* in *AtFH5* regulation, we crossed KS117, a GFP enhancer trap insertion at the *AtFH5* locus, with *taf13-2*. In KS117, the GFP signal can be detected in the endosperm starting at the stage of eight free endosperm nuclei. Before cellularization the GFP signal becomes weaker in the entire endosperm except for the chalazal region, to which expression is confined after cellularization, at least up to the bent-cotyledon stage of embryogenesis (Sorensen et al., 2001). In *fis* mutants, KS117 expression remains uniformly distributed in the entire endosperm at heart stage of embryogenesis (Sorensen et al., 2001). This was not observed in the *taf13-2* mutant where KS117 expression is normal from early stages of seed development (Fig. 5A and B) up to the cellularized endosperm stage, when expression was confined to the chalazal region like in wild type (n=403) (Fig. 5C and D). These results, based on this KS117 reporter line, suggest that TAF13 is not involved in the regulation of *AtFH5* and that the enlarged chalazal region in *taf13-2* mutant seeds does probably not depend on *AtFH5*.

To test a possible role of TAF13 in FIS-PRC2 target gene regulation, the expression of two other targets was analyzed. The *taf13-2* mutant was crossed with the *pPHE1*::*GUS* and *pFUS3*::*GUS* marker lines. *pPHE1*::*GUS* expression is detectable in embryo and endosperm soon after fertilization and persists until the heart stage of embryogenesis when endosperm cellularization occurs and the signal becomes restricted to the chalazal region (Kohler et al., 2003b). This expression pattern did not change in the *taf13-2* mutant (n=315) (Fig. 5E and F), whereas in the *mea* mutant, *PHE1* expression can be detected in the entire over-proliferating endosperm and embryo up to the heart stage

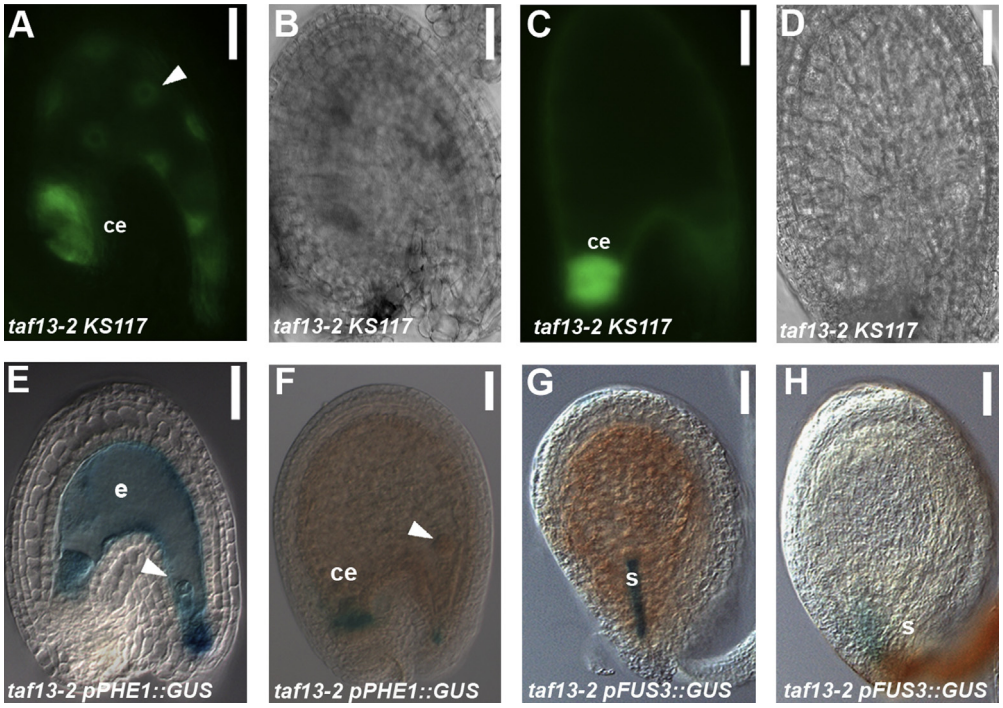

Fig. 5. *AtFH5*, *PHE* and *FUS3* expression in the *taf13-2* mutant. (A, B) GFP expression of enhancer trap at the *AtFH5* locus (*KS117* line) in *taf13-2* seeds (A) and its bright-field image (B) after the first rounds of mitotic endosperm divisions. The GFP signal is present in the chalazal endosperm region and in free endosperm nuclei (arrowhead). (C, D) GFP expression of KS117 in 5 DAP *taf13-2* seeds (C) and its bright-field image (D); the signal starts to be confined to the chalazal endosperm region. (E, F) *pPHE*::*GUS* expression in *taf13-2* at zygote embryo stage, with GUS staining in the embryo (arrowhead) and in the endosperm (E). (F) *pPHE*::*GUS* expression in *taf13-2* at 5 DAP is restricted to the chalazal region (arrowhead indicates the embryo). (G, H) *pFUS3*::*GUS* expression in *taf13-2* is confined to the suspensor when embryo development is already arrested at preglobular stage (G). *pFUS3*::*GUS* expression in *taf13-2* is still present in the suspensor of the degenerating embryo (H). Ce=chalazal endosperm; e=endosperm; s=suspensor. Scale bars 20 μm.

(Kohler et al., 2003b). *pFUS3*::*GUS* expression starts in the embryonic suspensor at the preglobular stage and it is present in the embryo until maturity (Kroj et al., 2003). In the *mea* mutant, *pFUS3*::*GUS* expression is altered showing GUS staining in the endosperm and embryo up to heart stage (Makarevich et al., 2006). Since *taf13-2* embryos are arrested at the preglobular stage, the signal in the embryo is detectable only in the suspensor (Fig. 5G). At later stages of endosperm development, no signal in the endosperm can be observed ($n=173$) (Fig. 5H), thus showing that also the *pFUS3*::*GUS* expression pattern was not changed in the *taf13-2* mutant.

Discussion

Our analysis shows that the TAF13 protein is nuclear expressed during all stages of embryo development, which is in agreement with its putative function as a transcriptional regulator. However, at later stages of embryo development, the TAF13 protein is especially in epidermis cells directed to the plasma membrane instead of the nucleus, suggesting an interesting post-translational regulatory mechanism. The fact that TAF13 does not seem to contain a Nuclear Localization Signal (NLS), suggests a piggyback mechanism for its transport to the nucleus and that in the epidermis cells of late stage embryos the TAF13 protein partner that guides transport to the nucleus might be missing. A similar scenario has been reported for human TAF10, which also lacks a NLS and its nuclear localization was shown to be dependent on its interaction partners (Soutoglou et al., 2005).

TAF13 is essential for embryo development since the *taf13-2* mutant displayed embryo arrest at the preglobular stage. Pol II activity studies during the first zygotic divisions in *Arabidopsis* showed a quiescent transcriptional state of the embryo (Pillot et al., 2010). Pol II-RNAi lines displayed embryo arrest at a preglobular stage, whereas endosperm development was blocked immediately after fertilization, suggesting a more active transcriptional state of this tissue (Pillot et al., 2010). These data suggest a differential role for *TAF13* in the two fertilization products, possibly explaining the ability of *taf13-2* mutant embryos to reach the preglobular stage, when *de novo* transcription is required and *TAF13* might be essential. However, more recent data revealed that, despite a slight delay in transcriptional activation compared to the endosperm, the embryo seems already to be transcriptionally active at very early stages (Nodine and Bartel, 2012). According to this scenario the observation that *taf13-2* mutant embryos reach the preglobular stage might be explained by the presence of a remainder TAF13 mRNA and/or protein from the parents. Alternatively TAF13 might not be essential until the globular stage.

The observed phenotype during endosperm development in *taf13-2* suggests a non-essential role in *de novo* transcription in this tissue. The over-proliferation of the chalazal endosperm, which is similar to the endosperm phenotype in *fis* mutants, and the interaction with the FIS-PRC2 components SWN and MEA, suggest a possible role of TAF13 in transcriptional regulation as a co-repressor. A role of TAFs in transcriptional repression is not unusual. Heterochromatin Protein 1 (HP1) is involved in heterochromatic gene silencing and was demonstrated to be stably associated with human TAF4 (Vassallo and Tanese, 2002). Moreover, *Drosophila* PRC1 interacts with 6 different TAFs and TBP (Saurin et al., 2001; Breiling et al., 2001) and transiently also with PRC2 components (Poux et al., 2001). It was also shown that GTFs are bound to *Polycomb*-repressed promoters, where Pol II is stalled and transcriptional initiation is blocked (Breiling et al., 2001; Dellino et al., 2004; Chopra et al., 2009). While chromatin packaging mediated by PcG proteins can block access to promoter regions, these data suggest an alternative repression mechanism,

where PcG proteins interact with GTFs to arrest transcriptional initiation (Dellino et al., 2004). A similar mechanism might also occur in plants, where FIS-PRC2-mediated transcriptional repression could be mediated by PcG protein binding to TFIID via TAF13. However, it is possible that other TAFs are required to accomplish this function since the expression analysis of three PRC2 targets in *taf13-2* mutant did not show the typical over-expression observed in *fis* mutants. The existence of different TFIID complexes (Jacq et al., 1994; Dikstein et al., 1996) and the fact that single TAFs may regulate only a subset of genes (Shen et al., 2003) could explain this result. In this work we focused our attention on the analysis of only three well-characterized FIS-PRC2 targets among the recently identified 1773 endosperm-specific target genes (Weinhofer et al., 2010). Therefore, it is possible that TAF13 is required for co-repression of a subset of targets, which does not include *PHE1*, *FUS3* and *AtFH5*, and that other TAFs might play redundant roles in the co-repression of these genes. According to publically available microarray data (Hruz et al., 2008) several *TAFs* are co-expressed with *TAF13* at medium/high levels in endosperm tissues, excluding *TAF1b*, *TAF4b*, *TAF8* and *TAF14b*, which are only low expressed. No expression data are available for *TAF5*, *TAF11b* and *TAF14*. Further analysis of the *taf13-2* mutant will be required to identify the genes that are regulated by a TAF13 containing FIS-PRC2 complex during endosperm development.

In conclusion, the data presented here support the hypothesis that TAF13 plays a role in FIS-PRC2-mediated repression and this might represent a promising step towards the understanding of the role that TAFs play in PcG-mediated transcriptional regulation in plants.

Acknowledgments

We thank D. Shubert (Heinrich-Heine Universität Düsseldorf) for helping with the yeast two-hybrid experiments; A. Chaudhury (Canberra, ACT, Australia) for the pFIS2::GUS and F. Berger (Temasek Lifesciences Laboratory, National University of Singapore, Singapore) for the KS117 enhancer trap line. This work was supported by the University of Zürich, a Grant of the Swiss National Science Foundation (to UG), a short-term EMBO Fellowship (ASTF No. 153-2010) and a travel Grant of the Company of Biologists (to ML), COST Action FA0903 (to UG), the EU project TransContainer (Food 2006 023018) (to MMK). ML and SS were supported by a PhD fellowship from the PhD school in Biomolecular Sciences, Università degli Studi di Milano.

Appendix A. Supporting information

Supplementary data associated with this article can be found in the online version at http://dx.doi.org/10.1016/j.ydbio.2013.03.005.

References

Alonso, J.M., Stepanova, A.N., Leisse, T.J., Kim, C.J., Chen, H., Shinn, P., Stevenson, D. K., Zimmerman, J., Barajas, P., Cheuk, R., Gadrinab, C., Heller, C., Jeske, A., Koesema, E., Meyers, C.C., Parker, H., Prednis, L., Ansari, Y., Choy, N., Deen, H., Geralt, M., Hazari, N., Hom, E., Karnes, M., Mulholland, C., Ndubaku, R., Schmidt, I., Guzman, P., Aguilar-Henonin, L., Schmid, M., Weigel, D., Carter, D.E., Marchand, T., Risseeuw, E., Brogden, D., Zeko, A., Crosby, W.L., Berry, C.C., Ecker, J.R., 2003. Genome-wide insertional mutagenesis of *Arabidopsis thaliana*. Science 301, 653–657.

Baroux, C., Gagliardini, V., Page, D.R., Grossniklaus, U., 2006. Dynamic regulatory interactions of *Polycomb* group genes: *MEDEA* autoregulation is required for imprinted gene expression in *Arabidopsis*. Genes Dev. 20, 1081–1086.

Basehoar, A.D., Zanton, S.J., Pugh, B.F., 2004. Identification and distinct regulation of yeast TATA box-containing genes. Cell 116, 699–709.

Bemer, M., Grossniklaus, U., 2012. Dynamic regulation of *Polycomb* group activity during plant development. Curr. Opinion Plant Biol.. [Epub ahead of print].

Bertrand, C., Benhamed, M., Li, Y.F., Ayadi, M., Lemonnier, G., Renou, J.P., Delarue, M., Zhou, D.X., 2005. *Arabidopsis HAF2* gene encoding TATA-binding protein (TBP)-associated factor TAF1, is required to integrate light signals to regulate gene expression and growth. J. Biol. Chem. 280, 1465–1473.

Bleckmann, A., Weidtkamp-Peters, S., Seidel, C.A., Simon, R., 2010. Stem cell signaling in *Arabidopsis* requires CRN to localize CLV2 to the plasma membrane. Plant Physiol. 152, 166–176.

Brambilla, V., Battaglia, R., Colombo, M., Masiero, S., Bencivenga, S., Kater, M.M., Colombo, L., 2007. Genetic and molecular interactions between BELL1 and MADS box factors support ovule development in *Arabidopsis*. Plant Cell 19, 2544–2556.

Bratzel, F., Lopez-Torrejon, G., Koch, M., Del Pozo, J.C., Calonje, M., 2010. Keeping cell identity in *Arabidopsis* requires PRC1 RING-finger homologs that catalyze H2A monoubiquitination. Curr. Biol. 20, 1853–1859.

Breiling, A., Turner, B.M., Bianchi, M.E., Orlando, V., 2001. General transcription factors bind promoters repressed by *Polycomb* group proteins. Nature 412, 651–655.

Chanvivattana, Y., Bishopp, A., Schubert, D., Stock, C., Moon, Y.H., Sung, Z.R., Goodrich, J., 2004. Interaction of *Polycomb*-group proteins controlling flowering in *Arabidopsis*. Development 131, 5263–5276.

Chaudhury, A.M., Ming, L., Miller, C., Craig, S., Dennis, E.S., Peacock, W.J., 1997. Fertilization-independent seed development in *Arabidopsis thaliana*. Proc. Natl. Acad. Sci. USA 94, 4223–4228.

Chen, D., Molitor, A., Liu, C., Shen, W.H., 2010. The *Arabidopsis* PRC1-like ring-finger proteins are necessary for repression of embryonic traits during vegetative growth. Cell Res. 20, 1332–1344.

Chopra, V.S., Hendrix, D.A., Core, L.J., Tsui, C., Lis, J.T., Levine, M., 2009. The *Polycomb* group mutant *esc* leads to augmented levels of paused Pol II in the *Drosophila* embryo. Mol. Cell 42, 837–844.

Clough, S.J., Bent, A.F., 1998. Floral dip: a simplified method for *Agrobacterium*-mediated transformation of *Arabidopsis thaliana*. Plant J. 16, 735–743.

Dellino, G.I., Schwartz, Y.B., Farkas, G., McCabe, D., Elgin, S.C., Pirrotta, V., 2004. *Polycomb* silencing blocks transcription initiation. Mol. Cell 13, 887–893.

De Lucia, F., Crevillen, P., Jones, A.M., Greb, T., Dean, C., 2008. A PHD-*Polycomb* Repressive Complex 2 triggers the epigenetic silencing of *FLC* during vernalization. Proc. Natl. Acad. Sci. USA 105, 16831–16836.

Demeny, M.A., Soutoglou, E., Nagy, Z., Scheer, E., Janoshazi, A., Richardot, M., Argentini, M., Kessler, P., Tora, L., 2007. Identification of a small TAF complex and its role in the assembly of TAF-containing complexes. PLoS One 2, e316.

Dikstein, R., Zhou, S., Tjian, R., 1996. Human TAFII 105 is a cell type-specific TFIID subunit related to hTAFII130. Cell 87, 137–146.

Dreni, L., Pilatone, A., Yun, D., Erreni, S., Pajoro, A., Caporali, E., Zhang, D., Kater, M. M., 2011. Functional analysis of all *AGAMOUS* subfamily members in rice reveals their roles in reproductive organ identity determination and meristem determinacy. Plant Cell 23, 2850–2863.

Egea-Cortines, M., Saedler, H., Sommer, H., 1999. Ternary complex formation between the MADS-box proteins SQUAMOSA, DEFICIENS and GLOBOSA is involved in the control of floral architecture in *Antirrhinum majus*. EMBO J. 18, 5370–5379.

Fitz Gerald, J.N., Hui, P.S., Berger, F., 2009. *Polycomb* group-dependent imprinting of the actin regulator *AtFH5* regulates morphogenesis in *Arabidopsis thaliana*. Development 136, 3399–3404.

Gao, X., Ren, F., Lu, Y.T., 2006. The *Arabidopsis* mutant *stg1* identifies a function for TBP-associated factor 10 in plant osmotic stress adaptation. Plant Cell Physiol. 47, 1285–1294.

Grant, P.A., Schieltz, D., Pray-Grant, M.G., Steger, D.J., Reese, J.C., Yates III, J.R., Workman, J.L., 1998. A subset of TAF(II)s are integral components of the SAGA complex required for nucleosome acetylation and transcriptional stimulation. Cell 94, 45–53.

Grossniklaus, U., Vielle-Calzada, J.P., Hoeppner, M.A., Gagliano, W.B., 1998. Maternal control of embryogenesis by *MEDEA*, a *Polycomb* group gene in *Arabidopsis*. Science 280, 446–450.

Hellens, R.P., Edwards, E.A., Leyland, N.R., Bean, S., Mullineaux, P.M., 2000. pGreen: a versatile and flexible binary Ti vector for *Agrobacterium*-mediated plant transformation. Plant Mol. Biol. 42, 819–832.

Hennig, L., Derkacheva, M., 2009. Diversity of *Polycomb* group complexes in plants: same rules, different players? Trends Genet. 25, 414–423.

Hiller, M.A., Lin, T.Y., Wood, C., Fuller, M.T., 2001. Developmental regulation of transcription by a tissue-specific TAF homolog. Genes Dev. 15, 1021–1030.

Holec, S., Berger, F., 2012. *Polycomb* group complexes mediate developmental transitions in plants. Plant Physiol. 158, 35–43.

Hruz, T., Laule, O., Szabo, G., Wessendorp, F., Bleuler, S., Oertle, L., Widmayer, P., Gruissem, W., Zimmermann, P., 2008. Genevestigator v3: a reference expression database for the meta-analysis of transcriptomes. Adv. Bioinformatics 2008, 420747.

Ingouff, M., Fitz Gerald, J.N., Guerin, C., Robert, H., Sorensen, M.B., Van Damme, D., Geelen, D., Blanchoin, L., Berger, F., 2005. Plant formin *AtFH5* is an evolutionarily conserved actin nucleator involved in cytokinesis. Nat. Cell Biol. 7, 374–380.

Jacq, X., Brou, C., Lutz, Y., Davidson, I., Chambon, P., Tora, L., 1994. Human TAFII30 is present in a distinct TFIID complex and is required for transcriptional activation by the estrogen receptor. Cell 79, 107–117.

Kohler, C., Hennig, L., Bouveret, R., Gheyselinck, J., Grossniklaus, U., Gruissem, W., 2003a. Arabidopsis MSI1 is a component of the MEA/FIE Polycomb group complex and required for seed development. EMBO J. 22, 4804–4814.

Kohler, C., Hennig, L., Spillane, C., Pien, S., Gruissem, W., Grossniklaus, U., 2003b. The Polycomb-group protein MEDEA regulates seed development by controlling expression of the MADS-box gene PHERES1. Genes Dev. 17, 1540–1553.
Kroj, T., Savino, G., Valon, C., Giraudat, J., Parcy, F., 2003. Regulation of storage protein gene expression in *Arabidopsis*. Development 130, 6065–6073.
Lago, C., Clerici, E., Dreni, L., Horlow, C., Caporali, E., Colombo, L., Kater, M.M., 2005. The *Arabidopsis* TFIID factor AtTAF6 controls pollen tube growth. Dev. Biol. 285, 91–100.
Lago, C., Clerici, E., Mizzi, L., Colombo, L., Kater, M.M., 2004. TBP-associated factors in *Arabidopsis*. Gene 342, 231–241.
Lawit, S.J., O'Grady, K., Gurley, W.B., Czarnecka-Verner, E., 2007. Yeast two-hybrid map of *Arabidopsis* TFIID. Plant Mol. Biol. 64, 73–87.
Lee, T.I., Causton, H.C., Holstege, F.C., Shen, W.C., Hannett, N., Jennings, E.G., Winston, F., Green, M.R., Young, R.A., 2000. Redundant roles for the TFIID and SAGA complexes in global transcription. Nature 405, 701–704.
Liljegren, S.J., Ditta, G.S., Eshed, Y., Savidge, B., Bowman, J.L., Yanofsky, M.F., 2000. *SHATTERPROOF* MADS-box genes control seed dispersal in *Arabidopsis*. Nature 404, 766–770.
Luo, M., Bilodeau, P., Dennis, E.S., Peacock, W.J., Chaudhury, A., 2000. Expression and parent-of-origin effects for *FIS2*, *MEA*, and *FIE* in the endosperm and embryo of developing *Arabidopsis* seeds. Proc. Natl. Acad. Sci. USA 97, 10637–10642.
Luo, M., Bilodeau, P., Koltunow, A., Dennis, E.S., Peacock, W.J., Chaudhury, A.M., 1999. Genes controlling fertilization-independent seed development in *Arabidopsis thaliana*. Proc. Natl. Acad. Sci. USA 96, 296–301.
Makarevich, G., Leroy, O., Akinci, U., Schubert, D., Clarenz, O., Goodrich, J., Grossniklaus, U., Kohler, C., 2006. Different *Polycomb* group complexes regulate common target genes in *Arabidopsis*. EMBO Rep. 7, 947–952.
Martinez, E., Kundu, T.K., Fu, J., Roeder, R.G., 1998. A human SPT3–TAFII31–GCN5-L acetylase complex distinct from transcription factor IID. J. Biol. Chem. 273, 23781–23785.
Nodine, M.D., Bartel, D.P., 2012. Maternal and paternal genomes contribute equally to the transcriptome of early plant embryos. Nature 482, 94–97.
Ogryzko, V.V., Kotani, T., Zhang, X., Schiltz, R.L., Howard, T., Yang, X.J., Howard, B.H., Qin, J., Nakatani, Y., 1998. Histone-like TAFs within the PCAF histone acetylase complex. Cell 94, 35–44.
Oh, S., Park, S., van Nocker, S., 2008. Genic and global functions for Paf1C in chromatin modification and gene expression in *Arabidopsis*. PLoS Genet. 4, e1000077.
Ohad, N., Margossian, L., Hsu, Y.C., Williams, C., Repetti, P., Fischer, R.L., 1996. A mutation that allows endosperm development without fertilization. Proc. Natl. Acad. Sci. USA 93, 5319–5324.
Ohad, N., Yadegari, R., Margossian, L., Hannon, M., Michaeli, D., Harada, J.J., Goldberg, R.B., Fischer, R.L., 1999. Mutations in *FIE*, a WD *Polycomb* group gene, allow endosperm development without fertilization. Plant Cell 11, 407–416.
Pillot, M., Baroux, C., Vazquez, M.A., Autran, D., Leblanc, O., Vielle-Calzada, J.P., Grossniklaus, U., Grimanelli, D., 2010. Embryo and endosperm inherit distinct chromatin and transcriptional states from the female gametes in *Arabidopsis*. Plant Cell 22, 307–320.
Poux, S., Melfi, R., Pirrotta, V., 2001. Establishment of *Polycomb* silencing requires a transient interaction between PC and ESC. Genes Dev. 15, 2509–2514.
Raissig, M.T., Baroux, C., Grossniklaus, U., 2011. Regulation and flexibility of genomic imprinting during seed development. Plant Cell 23, 16–26.
Saurin, A.J., Shao, Z., Erdjument-Bromage, H., Tempst, P., Kingston, R.E., 2001. A *Drosophila Polycomb* group complex includes Zeste and dTAFII proteins. Nature 412, 655–660.
Schatlowski, N., Creasey, K., Goodrich, J., Schubert, D., 2008. Keeping plants in shape: *Polycomb*-group genes and histone methylation. Semin. Cell Dev. Biol. 19, 547–553.
Shen, W.C., Bhaumik, S.R., Causton, H.C., Simon, I., Zhu, X., Jennings, E.G., Wang, T.H., Young, R.A., Green, M.R., 2003. Systematic analysis of essential yeast TAFs in genome-wide transcription and preinitiation complex assembly. EMBO J. 22, 3395–3402.
Sorensen, M.B., Chaudhury, A.M., Robert, H., Bancharel, E., Berger, F., 2001. *Polycomb* group genes control pattern formation in plant seed. Curr. Biol. 11, 277–281.
Soutoglou, E., Demény, M.A., Scheer, E., Fienga, G., Sassone-Corsi, P., Tora, L., 2005. The nuclear import of TAF10 is regulated by one of its three histone fold domain-containing interaction partners. Mol. Cell Biol. 25, 4092–4104.
Spillane, C., Baroux, C., Escobar-Restrepo, J.M., Page, D.R., Laoueille, S., Grossniklaus, U., 2004. Transposons and tandem repeats are not involved in the control of genomic imprinting at the *MEDEA* locus in *Arabidopsis*. Cold Spring Harbor Symp. Quant. Biol. 69, 465–475.
Spillane, C., Schmid, K.J., Laoueille-Duprat, S., Pien, S., Escobar-Restrepo, J.M., Baroux, C., Gagliardini, V., Page, D.R., Wolfe, K.H., Grossniklaus, U., 2007. Positive darwinian selection at the imprinted *MEDEA* locus in plants. Nature 448, 349–352.
Tamada, Y., Nakamori, K., Nakatani, H., Matsuda, K., Hata, S., Furumoto, T., Izui, K., 2007. Temporary expression of the TAF10 gene and its requirement for normal development of *Arabidopsis thaliana*. Plant Cell Physiol. 48, 134–146.
Thomas, M.C., Chiang, C.M., 2006. The general transcription machinery and general cofactors. Crit. Rev. Biochem. Mol. Biol. 41, 105–178.
Vassallo, M.F., Tanese, N., 2002. Isoform-specific interaction of HP1 with human TAFII130. Proc. Natl. Acad. Sci. USA 99, 5919–5924.
Vielle-Calzada, J.P., Thomas, J., Spillane, C., Coluccio, A., Hoeppner, M.A., Grossniklaus, U., 1999. Maintenance of genomic imprinting at the *Arabidopsis MEDEA* locus requires zygotic *DDM1* activity. Genes Dev. 13, 2971–2982.
Vinkenoog, R., Spielman, M., Adams, S., Fischer, R.L., Dickinson, H.G., Scott, R.J., 2000. Hypomethylation promotes autonomous endosperm development and rescues postfertilization lethality in *fie* mutants. Plant Cell 12, 2271–2282.
Voinnet, O., Rivas, S., Mestre, P., Baulcombe, D., 2003. An enhanced transient expression system in plants based on suppression of gene silencing by the p19 protein of tomato bushy stunt virus. Plant J. 33, 949–956.
Voronina, E., Lovasco, L.A., Gyuris, A., Baumgartner, R.A., Parlow, A.F., Freiman, R.N., 2007. Ovarian granulosa cell survival and proliferation requires the gonad-selective TFIID subunit TAF4b. Dev. Biol. 303, 715–726.
Wang, D., Tyson, M.D., Jackson, S.S., Yadegari, R., 2006. Partially redundant functions of two SET-domain *Polycomb*-group proteins in controlling initiation of seed development in *Arabidopsis*. Proc. Natl. Acad. Sci. USA 103, 13244–13249.
Weinhofer, I., Hehenberger, E., Roszak, P., Hennig, L., Kohler, C., 2010. H3K27me3 profiling of the endosperm implies exclusion of *Polycomb* group protein targeting by DNA methylation. PLoS Genet. 6, e1001152.
Wieczorek, E., Brand, M., Jacq, X., Tora, L., 1998. Function of TAF(II)-containing complex without TBP in transcription by RNA polymerase II. Nature 393, 187–191.
Wood, C.C., Robertson, M., Tanner, G., Peacock, W.J., Dennis, E.S., Helliwell, C.A., 2006. The *Arabidopsis thaliana* vernalization response requires a *Polycomb*-like protein complex that also includes VERNALIZATION INSENSITIVE 3. Proc. Natl. Acad. Sci. USA 103, 14631–14636.
Zhang, X., Clarenz, O., Cokus, S., Bernatavichute, Y.V., Pellegrini, M., Goodrich, J., Jacobsen, S,E., 2007. Whole-genome analysis of histone H3 lysine 27 trimethylation in *Arabidopsis*. PLoS Biol. 5, e129.